Available online at www.sciencedirect.com
SCIENCE DIRECT®

Journal of the European Ceramic Society 23 (2003) 2993–2999
www.elsevier.com/locate/jeurceramsoc

Unmelted particles in plasma sprayed coatings

Pavel Ctibor[a,*], Olivier Roussel[b], Aurelien Tricoire[b]

[a]*Institute of Plasma Physics ASCR, Czech Republic*
[b]*National Higher Engineering School of Limoges (ENSIL), Limoges, France*

Received 7 August 2002; received in revised form 23 January 2003; accepted 1 February 2003

Abstract

A technique is described for investigation of unmelted particles in plasma spraying and for porosity investigation in coatings. A study of unmelted particles is made. The technique is based on large area section (LAS) images, superimposed to obtain a densely packed "column" of images as a 3-D map of a certain volume of the plasma sprayed coating. Optical micrographs of a polished cross section of the coating were used. The LAS technique combines two parameters—magnification and field size. Such a combination is normally beyond the range of optical microscopy. The method makes it necessary to polish the sample again and again and after each polishing step align precisely the new LAS with the previous one. The unmelted particles are considered to have been spheroidized in the plasma plume during plasma spraying, but to have cooled below the melting point before reaching the substrate. Such particles are embedded in the coating as previously solidified, i.e. with globular shape. The 3-D map makes it possible to observe their distribution inside the coating. These globular particles represent defects in the deposited coating. Moreover they have a tendency to behave isotropically under the influence of stress or other physical factors and in this way serve in the anisotropic structure of the coating as centers of secondary defects deteriorating the functional properties of the coatings.

Keywords: Defects; Optical microscopy; Plasma spraying; Structural applications; Titanates

1. Introduction

The 3-D map technique was originally developed on biological samples by means of refocusing the microscope inside the depth within the sample. The "seaming" of single micrographs to create Large Area Sections (LAS) has been long used. Tewari[1] demonstrated the use of LASs for 3-D maps. The technique is also useful for metallography and the observation of nontransparent solid samples. It has not been used in the field of plasma spraying to study the sprayed coating structure.

We accordingly adopt part of the technique used by Tewari.[1] This employs a "dissector" for the stereological interpretation of the 3-D microstructure. The dissector includes two parallel sectioning planes separated by a known distance.

In opaque microstructures, application of the dissector requires the storing of a micrograph of an arbitrary field of view on the first dissector plane, the physical removal of a known small thickness of material by polishing followed by a suitable image analysis procedure to determine how many features, selected by the counting frame placed on the micrograph on the first plane, are not present on the second sectioning plane. In this process most of the effort goes into the specimen preparation steps, such as physical sectioning, polishing of LASs planes, identification of the same microstructural region on the two sectioning planes and measurement of the thickness (i.e. distance between neighboring LASs) of the material removed. The number of counted microstructural elements can be increased by observing the structure at a much lower magnification. This is often not acceptable because loss of resolution can lead to significant measurement errors. To obtain high resolution in conventional microscopy techniques, the structure is observed at high magnification, and that decreases the area of the field of view, which is inversely proportional to the square of the magnification. A large-area dissector (LAD) has been proposed by Tewari[1] as a solution to this problem. In LAD the dissectors have a very large area and a very

* Corresponding author. Tel.: +420-2-66-05-37-27; fax: +420-2-85-86-389.
E-mail address: ctibor@ipp.cas.cz (P. Ctibor).

0955-2219/03/$ - see front matter © 2003 Elsevier Ltd. All rights reserved.
doi:10.1016/S0955-2219(03)00104-3

high resolution. The edges of the LAD are hundreds of dissector thicknesses. The dissector planes (in our work, which does not need the stereological implication of the term ''dissector,'' the term ''large area section—LAS'' is used for a zone of interest on a single plane) consist of a ''montage'' of a very large number of contiguous microstructural fields of view taken at high magnification and precisely ''pasted'' together by an interactive image analysis procedure. Therefore, for about the same metallographic effort, the LAS can yield many times larger particle counts or pore counts than conventional single field of view micrographs.

2. The technique

2.1. Material selection and sample manufacturing

Titanates, in general, form a wide and important group of technical ceramics. Besides titanium oxide itself, the ternary systems, $ATiO_3$, represent the simplest titanate materials used for technical applications. Interesting properties can be found in ilmenite-type crystals such as is $MgTiO_3$. A mixture of $MgTiO_3$ and $CaTiO_3$, with Mg:Ca ratio equal to 94:6 (label MCT) was plasma sprayed at the Institute of Plasma Physics ASCR, Prague, Czech Republic and studied from different aspects.[2–6] It was proved that the microstructure of a MCT plasma deposit is representative enough to serve as a pilot material for studying the microstructure of plasma deposits in general.

Samples were manufactured using a high-throughput water-stabilized plasma spray system WSP© PAL 160 (Institute of Plasma Physics, Prague, Czech Republic). This system operates at about 160 kW arc power and can process high amounts of material per hour. In the current experiment, feedstock throughputs of 22–24 kg/h were used, i.e. about 50% of the maximum available throughput of this system. The spray parameters—feeding distance and spray distance—were optimized by testing single splat shapes and sizes before deposition of the samples. Feeding distance (FD) 24 mm spraying distance (SD) 360 mm were used to spray present sample. Optimum preheating temperature of the substrate was also identified as 300 °C and used at sample manufacturing. As substrates, flat carbon steel as well as stainless steel samples were used. The feedstock size was 63–125 microns. Powder was fed in by compressed air through two injectors. The deposited thickness was about 1 mm, the covering of entire substrate by the coating was maintained by the automatic manipulator handling with the spray gun.

The metal substrate covered by plasma sprayed MCT coating was cut by a low speed saw equipped with a diamond wheel (Leco, USA). A cross section of the substrate-coating system was mounted in resin to create a classical metallographic section. Then grinding was completed with a rough grain diamond paste (Struers, Denmark) on an automatic metallographic grinding machine (Wirtz, Gemany). Polishing of individual planes for large area section imaging was performed manually using diamond polishing paste with grain size 1 μm.

2.2. Creation of the large-area section

This involved a sequence of steps, namely:

1. Identification of a suitable large region on the first cross section plane covering 25 microstructural fields of view and the ''tagging'' of this region by placing two microhardness indents in the metal substrate near the substrate-coating interface in the known distance from the selected region border.
2. Creation of a seamless ''montage'' covering all microstructural fields in this region of the first plane.
3. Physical removal of a small amount of material by polishing, identification of the same region on the second plane by using positions of microhardness indents as the point of reference.
4. Creation of a seamless montage of all microstructural fields of view of the same region on the second plane.
5. Measurement of the distance between the subsequent planes by measuring the decrease in the sizes of the microhardness indents on the second plane.
6. Creation of new indents in the same places as previously, measuring their dimensions and repeating the whole procedure.

2.3. Microstructural montage

To create the montage, the first field of view can be chosen at any one corner of the region of interest. The high magnification image of this field of view is then stored in the memory of the image analysis computer as an image file. After that the specimen is manually shifted by movement of the microscope stage, the shift being controlled by observation of the live image on the screen. After a perfect alignment of the border of the previously stored and the new live image, this live image is stored in the computer memory as another image file. All successive images are captured by using the same procedure until finally a continuous montage of the whole region of interest is created. The montage is essentially a microstructural image of a large area (25 fields of view at ×800 magnification in this case) having high resolution (~0.4 μm). Fig. 1 shows an example of a LAS obtained in the described way.

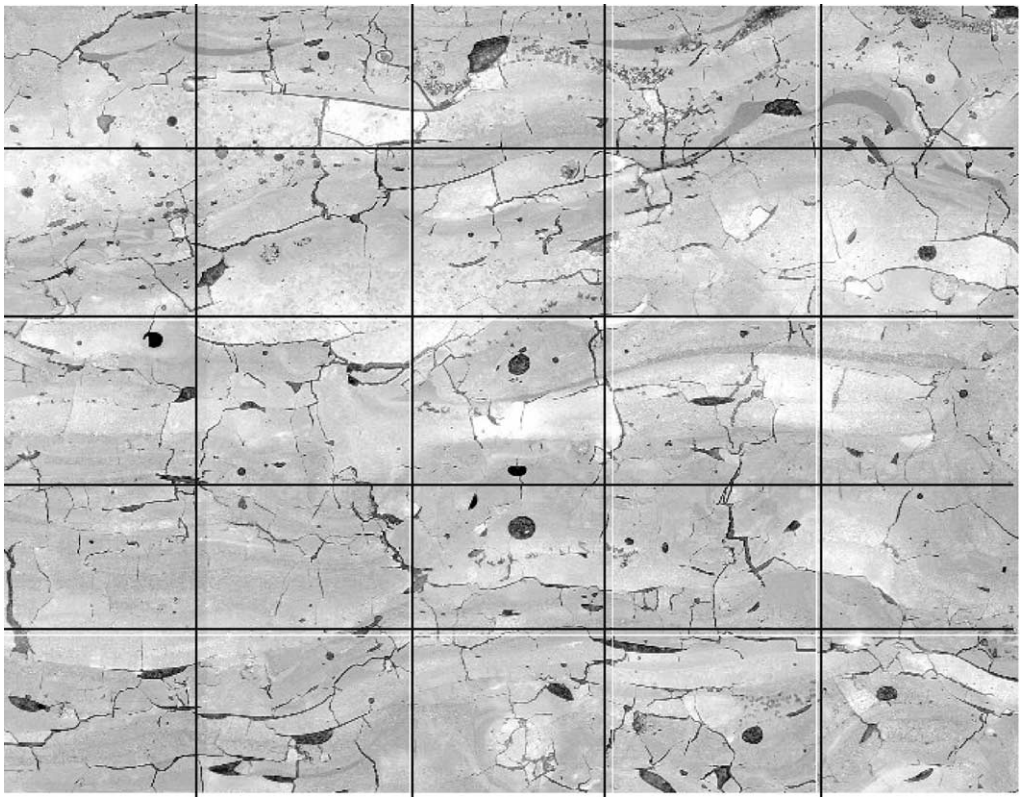

Fig. 1. Large area section No. 5 with scheme of the grid between single images.

2.4. Generation of the subsequent LAS and alignment of LASs

After creation of the montage on the first plane, the specimen is removed from the microscope stage. The specimen is then polished to remove approximately 3 μm of thickness from the material. This process prepares the second plane for the creation of the second large area section. The microhardness indents are used to align the two subsequent planes. There exists some translational and rotational displacement of one LAS with respect to the previous one. In the present study we achieved translational displacement of about 3 μm and rotational displacement of approximately 3 angular degrees. Such inaccuracy is unavoidable with our equipment using this technique. We control precisely not only the neighboring LASs but also the next nearest neighbors to avoid the summation of the inaccuracy in any one direction—either translational or rotational.

We used the Neophot 32 microscope (Zeiss, Germany) and Lucia G3.52a image analysis software (Laboratory Imaging, Czech Republic) for capturing the images and for creation of the LAS. The combination of the resolution in one LAS (0.4 μm) and the distance between LASs (3 μm) was selected with respect to the main structural features of plasma sprayed coatings.

2.5. Measurement of distance between two neighboring LASs

For any stereological measurements in the 3-D map of the structure, one needs to know the distance between two neighboring LASs. This distance can be calculated by measuring the decrease in the size of the microhardness indents. Therefore the indents in the metallic substrate have two functions. They serve as tagging markers for the alignment of images and also for the measurement of the depth of material removal by means of polishing. The indents were made by a square pyramidal shaped diamond indenter with opposite faces at an angle of 136°, where the ratio of the diagonal of the square formed on the section to the depth is equal to 7.00. Thus for a unit change in diagonal length there was 1/7 change in the depth. The change in the size of each microhardness indent can be measured by using image analysis, and the average distance between the two LASs can be calculated from these data.

2.6. Construction of large volume of microstructure (3-D map)

To build a 3-D map of the microstructure, the serial sectioning was continued beyond the second plane and 80 montage serial sections were created, each consisting

of a montage of 25 microstructural fields, by using exactly this same procedure. A 3-D microstructural volume can be recreated from such closely spaced serial sections by using 3-D image processing. We used the 3-D image analysis software by Voxblast 3.0 (VayTek, USA). The method from starting to store the images to the 3-D image rendering is best named the Volume Reconstruction (VR) method.

Fig. 2 shows a rendering of the 3-D map with labeling of axes, with the notation for single image nomenclature and with the orientation towards the spray gun and substrate.

3. The unmelted particles

3.1. Origin and characteristics

The work[7] was concentrated on a structural examination of MCT as-sprayed plasma deposits. This material, like the majority of ceramics used in plasma spraying, exhibits a lamellar microstructure after spraying. All regions of the studied volume exhibiting deviations from such lamellar character are in the focus of the current work.

The 3-D map based on LASs gives us the possibility to observe the distribution of such regions inside the studied space of the coating. The "unmelted" globular particles inside the lamellar structure of the deposit serve as sources of defects created during the spraying and cooling of the deposited coating. Moreover they have a tendency to behave isotropically under the influence of stress or other physical factors and thus serve, in the anisotropic structure of the coating, as centers of secondary defects degrading the functional properties of the coatings.

3.2. Feedstock manufacturing

Another interesting fact is that unmelted particles retain some structural features reflecting their "history". In the case of the studied material, MCT, this history consists of the following steps:

1. Mixing and homogenization of powders of $MgTiO_3$ and $CaTiO_3$ having size approximately 5–15 μm (so called "micropowder").
2. Mixing the resulting powder with an organic plastifier and the shaping of tablets.
3. Calcination of the tablets to remove the plastifier together with moisture to obtain chemical bonding between the grains of the powder.
4. Sintering of the tablets to obtain "dense" bulk ceramics.
5. Crushing the tablets and sieving the resulting powder to obtain the proper size distribution for spraying.

Steps 1–4 represent the "classical" manufacturing procedure for the fabrication of bulk ceramics. For the

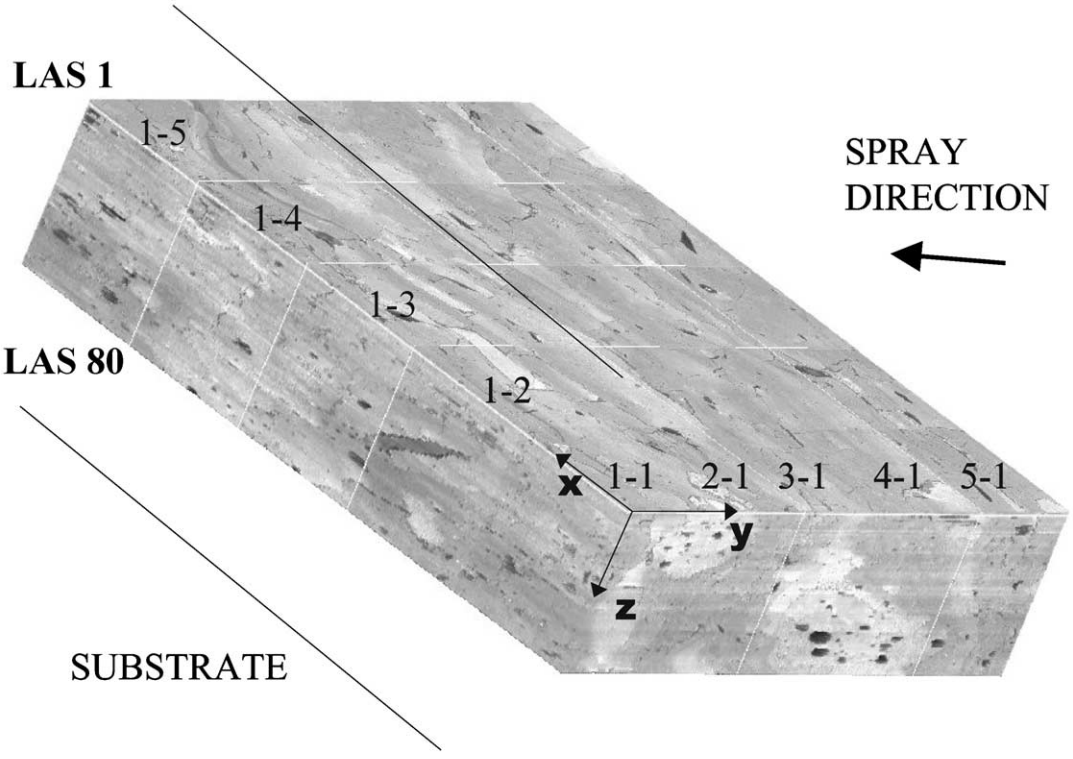

Fig. 2. Surface rendered 3-D reconstruction of studied volume.

spraying of common materials like alumina, commercially available fused and crushed powders are universally used. But other materials such as titanates are seldom available on the market in conditions useful for spraying. For experimental purposes, the MCT material was sprayed as powder prepared from commercial bulk ceramics. As will be shown in the experimental part of this paper, unmelted particles embedded in the deposit are strongly influenced by the original microstructure of the bulk precursor.

4. Experimental

In the studied volume two different kinds of unmelted particles were found. One of them is a particle having approximately globular shape and a sharp border. These can be termed US—unmelted spherules. The second type has a complicated shape and a smeared border. These can be termed DZ—diffusive zones. Both types are marked in Fig. 3, where the numbers 1–3 correspond to US, and numbers 4 and 5 to DZ. The investigation of unmelted particles must be done manually, because it is impossible to threshold them with image analysis software.

With US, the size was measured in two directions—particle "diameter" and "thickness." On the X–Y plane, each particle was observed on subsequent large area sections and the largest section of the particle was measured. The average of diameters X and Y was considered as a particle sectional "diameter." On the Z level, the number of LASs containing each particle was counted and multiplied by the average distance between LASs. The "thickness" is obtained in this way. Also it is obvious that the sources of uncertainty in the two parameters are markedly different. For simplification, we will now consider the US as perfect globes.

With regard to DZ only the "thickness" can be measured properly. The same approach was used as in the case of US.

5. Size, number and volume fraction of unmelted particles

Fig. 4 shows the largest unmelted particle present in the studied volume. The particle is not completely inside the studied volume (left border of Fig. 4 is the edge of the studied volume; see also Fig. 2—the bottom edge below the label 4-1).

The estimated diameter of this particle is minimally 183 μm and it belongs to the DZ type because it is connected with the unmelted zone on the top of the image.

In the entire volume studied 28 objects of the US type were found. Their average diameter is 21.2 μm and the average thickness is 19.5 μm. Also the consideration of their globularity could be brought into the calculations. Their total volume is 6618 μm^3.

Also in the whole volume studied 18 objects of the DZ type were found. Their average thickness is 68.0 μm. If we try to calculate their total volume considering their shape as globular (which is not as valid as in the case of US), the total volume is 1.5×10^6 μm^3.

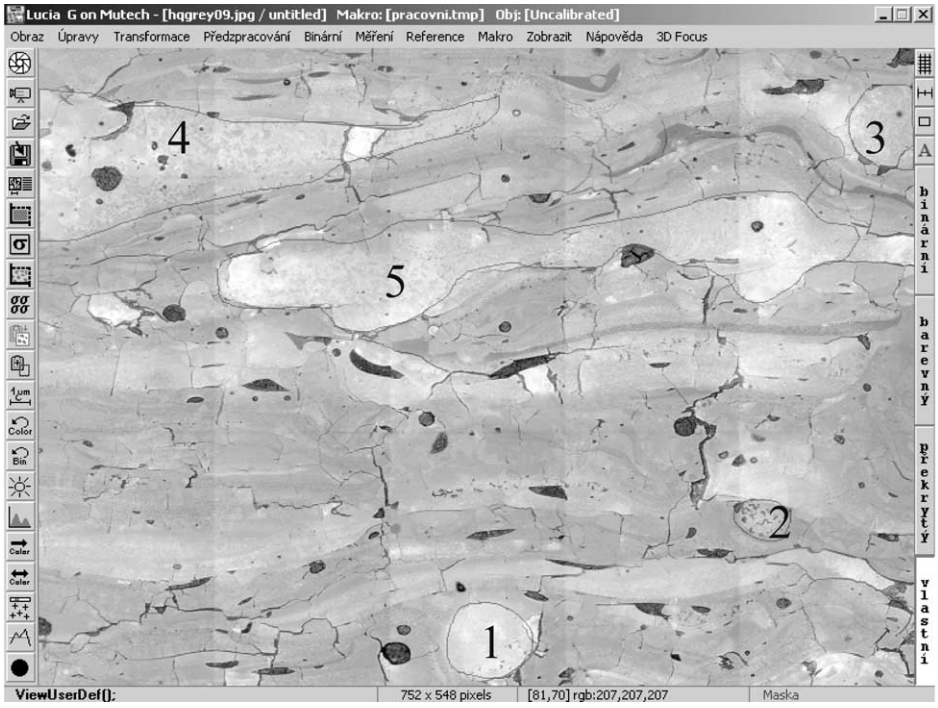

Fig. 3. Screen of image analysis software with numbered particles.

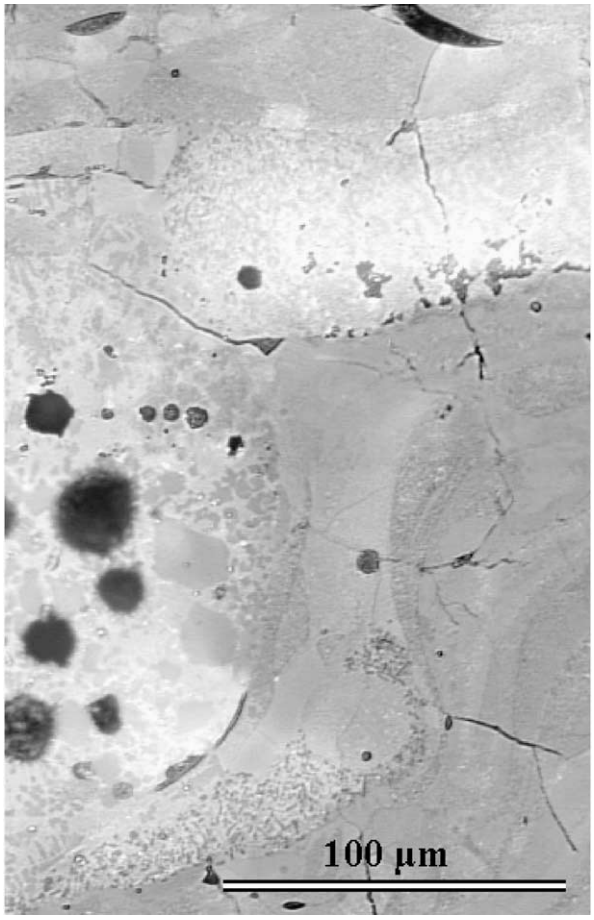

Fig. 4. Part of the largest unmelted particle detected in the studied volume.

Both types of unmelted particles embraced together 0.001574 mm^3, which is 4.37% of the studied volume.

It is interesting to compare the volume fraction, the area fraction of certain LAS, the area fraction of certain single images and also the line fractions for the unmelted particles. This comparison could be completed for US-type only because these particles have a convex shape. As a result, an absolute volume fraction and an area fraction on randomly selected LAS as well as an area fraction on randomly selected single image and a line fraction on randomly selected lines parallel to the x-axis in certain LAS would be used. Table 1 shows the results.

The content of Table 1 is based on Crofton law from integral geometry expressed by the equation $V_v = A_a$. Here V_v is volume fraction of studied objects and it is a constant, A_a is area fraction and it represents mean value over all planes going through the studied volume (all orientations and translations theoretically; planparallel system of planes in our case). Similar rules can be applied at reduction of studied volume to lines or points interacting with unmelted particles inside studied volume. From Table 1 it is evident that the area fraction of LAS has a similar value to the volume fraction. On the other hand, the area fraction of a single image has a value one order of magnitude higher as also for the line fraction. There is complicated (and Table 1 does not include this point of view) to obtain a set of single images or single lines providing mean value representative enough in the sense of Crofton law. This comparison supports the importance of the LAS in microstructural investigations.

From the point of view of unmelted particles we can see that they represent 0.7% of the sample volume (US type alone) or 4.37% (US together with DZ type).

6. Spacing of unmelted particles

The spacing of unmelted particles was studied using the "Index of dispersion test"[8] belonging to the Quadrate counts methods.[8] The index of dispersion I is defined by

$$I = (k-1)s^2/x' \quad (1)$$

where k is the number of quadrates, x' is the mean number of points per quadrate and s^2 is the sample variance of the number of points per quadrate. This test statistic is exactly that of a χ^2 goodness of fit test of the hypothesis that the n points are independently and uniformly distributed in studied volume. If the index I is not equal to $\chi^2_{k-1;\alpha}$ then the test rejects the stationary Poisson point process hypothesis at significance level $100\alpha\%$.

We divide our studied volume into 12 quadrates of the same size and each unmelted particle of US-type is represented by its central point. Also we obtain $k = 12$, $x' = 2.3$, $s^2 = 1.055$ and $I = 4.97$.

Corresponding $\chi^2_{k-1;\alpha}$ is 19.67 for $\alpha = 5\%$. Also I is smaller than $\chi^2_{k-1;\alpha}$ and it means that there exists some regularity in the point pattern as the variability is smaller that for the Poisson process.

Therefore we can conclude that the spacing of unmelted particles (of US type) is not random. Manual operation with LAS pictures and observation of unmelted particles seem to lead to the opinion that the

Table 1
Estimations of unmelted particle fractions in MCT material

Criterion	Volume fraction	Area fraction—LAS	Area fraction—single image	Line fraction
Region	3-D volume	LAS 27	LAS 43-2-2	LAS 27—line $Y = 60$ pixels
Value	0.0070	0.0087	0.057	0.071

spherical particles are slightly clustered together. Such a fact implies fluctuations in the process parameters, probably in a similar way to that described in.[9]

7. The difference between porosity in the overall plasma deposit and in the unmelted particles

Circularity (CI) describes the shape of pores on one section

$$\mathrm{CI} = 4\pi.AO/P^2, \quad (2)$$

where AO is the area of the pore and P is its perimeter. A perfect circle has circularity 1 and all the various shapes have the value between 0 and 1.

The circularity of all pores larger than approximately 2.5 μm is 0.53. When the measurement is made inside the unmelted particles only, it is 0.77. This result indicates that the pores inside the unmelted particles are more circular (globular) than in the general deposit. The high circularity/globularity is typical for sintered bulk ceramics. This fact reveals that the unmelted particles retain the porosity present in the powder, which was prepared from bulk material as described earlier.

8. Conclusions

Unmelted particles are serious defects in thermal spray coatings. They are almost unavoidable in plasma sprayed coatings. Some other techniques like High Velocity Oxy Fuel spraying or Cold spraying are favorable where metals are sprayed. Such techniques minimize the number of unmelted particles in the coating.[10] Their use is a possible solution for low-melting-point materials. For spraying ceramics it is necessary to accept a certain quantity of unmelted particles. The best procedure is then to know more about their occurrence and significance.

The VR method utilizing LAS and 3-D mapping was found to be useful for microstructural investigation in the field of plasma spraying. In the present work it was demonstrated by studying unmelted particles.

Typical unmelted particles are dominantly spheroidal and exhibit a microstructure that is firmly connected with the process of powder fabrication before spraying. If sintered powder is used, the grain and pore shape of the originally sintered ceramics is present in the unmelted particles. The thermal history of the powder probably bears the responsibility for the presence of diffusive zones besides the "common" spheroidal particles (unmelted spherules). The spheroidal unmelted particles are not randomly distributed inside the coating but they seem to exhibit a certain clustering. This could be a consequence of fluctuations in the spray set-up parameters.

Acknowledgements

This work was supported by the Grant Agency of the Czech Republic under No. 104/01/0149. The authors wish to thank R. Jùzková (Department of Probability and Statistics, Faculty of Mathematics and Physics, Charles University, Praha, Czech Republic) for her help with statistical treatment of the particles spacing data.

References

1. Tewari, A. and Gokhale, A. M., Efficient estimation of number density in opaque material microstructures: the large area dissector. *Journal of Microscopy*. **200**(3) 277–283.
2. Ctibor, P. *et al*., Plasma spraying of titanates—I. In *Proceedings of the 1st International Thermal Spray Conference*, ed. C. Berndt. ASM International, Materials Park, OH, 2000, pp. 945–950.
3. Neufuss, K. and Rudajevova, A., Thermal properties of the plasma-sprayed $MgTiO_3$–$CaTiO_3$ and $CaTiO_3$. *Ceramics International*, 2002, **28**(1), 93–97.
4. Ctibor, P. and Sedlacek, J., Dielectric properties of plasma sprayed titanates. *Journal of European Ceramic Society*, 2001, **21**, 1685–1688.
5. Ctibor, P., *Study of Structure and Properties of Plasma Deposits of Perovskite-Related Ceramics*. PhD thesis, Czech Technical University, Prague, 2000 (in Czech).
6. Ctibor, P., Sedlacek, J., Neufuss, K. and Chraska, P., Dielectric relaxation in calcium titanate-containing ceramics prepared by plasma spraying. Ceramics International (accepted for publication).
7. Ctibor, P., Kolman, B. and Rohan, P., Chemical and microstructural changes in plasma sprayed $MgTiO_3$–$CaTiO_3$ system during subsequent annealing. In *Proceedings of the 4th European Microbeam Analysis Society Regional Workshop*, ed. V. Stary, K. Masek and K. Horak. FME, Czech Technical University, Prague, 2000, pp. 198.
8. Stoyan, D., Kendall, W. S. and Mecke, J., *Stochastic Geometry and its Applications*, 2nd edn. John Wiley & Sons, Chichester, 1995.
9. Bisson, J. F. and Moreau, C., Effect of DC plasma fluctuations on in-flight particle parameters—Part II. In *Proceedings of International Thermal Spray Conference 2002*, ed. C. Berndt, Essen, Germany, 2002, pp. 666–671.
10. Stoltenhoff, T., Voyer, J., and Kreye, H., Cold spray—state of the art and applicability. In *Proceedings of International Thermal Spray Conference 2002*. ed. C. Berndt, Essen, Germany, 2002, pp. 366–374.